

---

# Adversarial Noise Layer: Regularize Neural Network By Adding Noise

---

**Zhonghui You**<sup>†</sup>  
zhonghui@pku.edu.cn

**Jinmian Ye**<sup>‡</sup>  
jinmian.y@gmail.com

**Kunming Li**<sup>§</sup>  
u5580030@anu.edu.au

**Ping Wang**<sup>†</sup>  
pwang@pku.edu.cn

<sup>†</sup>School of Electronics Engineering and Computer Science, Peking University

<sup>‡</sup>University of Electronic Science and Technology of China

<sup>§</sup>Australian National University

## Abstract

In this paper, we introduce a novel regularization method called Adversarial Noise Layer (ANL), which significantly improve the CNN's generalization ability by adding adversarial noise in the hidden layers. ANL is easy to implement and can be integrated with most of the CNN-based models. We compared the impact of the different type of noise and visually demonstrate that adversarial noise guide CNNs to learn to extract cleaner feature maps, further reducing the risk of over-fitting. We also conclude that the model trained with ANL is more robust to FGSM and IFGSM attack. Code is available at: <https://github.com/youzhonghui/ANL>

## 1 Introduction

Although Convolutional Neural Networks (CNNs) are powerful and popularly used in various computer vision tasks, they suffer from over-fitting due to the excessive amount of parameters [22]. The initial development of the neural network is inspired by the mechanism of human brain [18] which does not work as precisely as the computer. Inspired by the difference, we infer that adding noise into the process of training could instruct CNNs to learn more robust feature representations to against the effect of noise, thereby reducing the risk of over-fitting.

Many regularization methods prevent over-fitting through adding noise into the training data [9, 21, 30, 1, 26]. Data augmentation of the input image such as random cropping, flipping, and blocking [9, 21, 30] has been widely used in improving the generalization ability of CNNs. Adversarial Training [1] was proposed to regularize the network through adding the gradient-based perturbation into the images. DisturbLabel [26] randomly changed the label of a small subset of samples to incorrect value each iteration, thereby regularizing the CNNs on loss layer.

Regularization methods by injecting noise into the hidden layers are also proposed [22, 24]. Hinton *et al.* introduced Dropout [22], which regularizes a large network by randomly mask the units with zero in the process of training. However, Dropout performs unsatisfactorily when it's integrated with batch normalization [7] which is regarded as a powerful skill and has been widely applied in CNNs.

In this work, we further propose a well compatible and applicable regularization method, which improves the robustness of CNNs obviously by injecting the well-designed noise into the network in training. We name the noise which is calculated based on the gradient as the adversarial noise since it's similar to the perturbation calculation in Adversarial Training [1].

Differ from Adversarial Training (AT), Adversarial Noise Layers (ANLs) add the noise to the input images as well as the hidden layers. In addition, ANL can be embedded into CNN models easily. We further explore the impact of different  $\epsilon$  and find that its value is related to the number of parameters in the network. It is only taking effect in the process of training when ANLs are embedded. So the ANL actually takes no extra computation in inference process. In summary, we make the contributions as follows:

- (a) We introduce a novel CNN regularization method called ANL that regularizes CNNs to learn more robust feature representations by injecting gradient-based noise into hidden layers. Empirical results show that ANL can significantly improve the performance of various mainstream deep convolution neural networks on popular datasets.
- (b) We demonstrate that ANL is well compatible with various CNNs architectures and can be injected without changing the design philosophy. In addition, ANL takes no extra computation for the network in inference process.
- (c) We verified the ANL are able to boost robustness of CNN models under the attack of Fast Gradient Sign Method [1] and Iterative Fast Gradient Sign Method [10]. With proper setting, ANL contributes to boosting robustness of CNN models under FGSM and IFGSM attack as well as enhancing the accuracy of clean data.

## 2 Related Work

The recent rapid progress of CNNs in computer vision tasks such as image classification, semantic segmentation [3] and image restoration [17] is partly due to the creation of large-scale dataset such as ImageNet [19] *etc.* It is commonly believed that robust models usually require large-scale sufficient training data set or expensive computation to avoid over-fitting [12]. Therefore, to overcome the over-fitting challenge, various methods and techniques are proposed such as optimization techniques [22], regularization methods and *etc.*

The early solutions for avoiding over-fitting is to constrain the parameters by using the  $\ell_2$  regularization [8] or to stop training before convergence [16]. Various regularization methods aim to reduce over-fitting are proposed recently. With a certain probability, the dropout method reduces over-fitting in large feed-forward neural networks by masking a random subset of the hidden neurons with zero during training [22] but performs unsatisfactorily in tiny or compact networks. DropConnect [24] randomly masks the weights with zero in training phase. Stochastic Pooling [28] changes the deterministic pooling operation with randomly selects activations according to a certain distribution during training.

Recently, regularization methods by adding noise are introduced [9, 21, 30]. Simonyan *et al.* [21] introduced the methods to avoid over-fitting by random horizontal flipping train data, which directly enlarge training dataset. Zhong *et al.* [30] and Krizhevsky *et al.* [9] further proposed data augmentation methods through erasing training and crop training dataset randomly. Adversarial Training [1] enlarged training data set by adding adversarial training data to reduce the model sensitivity and improve the robustness of CNN models. DisturbLabel [26] added noise at the loss layer through randomly changing the label of a small subset of samples to incorrect values during training, thereby regularizing the CNN models. Different from the methods mentioned above, our approach (ANL) regularizes CNN models by adding adversarial noise in hidden layers, learning more robust feature representations. ANL can be integrated easily into the most CNN-based models and obtain better performance.

## 3 Method

### 3.1 Terminology and Notation

To simplify, in this paper we use following notations and terminologies to illustrate our algorithm:

1.  $J(\mathbf{x}, y; \boldsymbol{\theta})$  denotes the cost function used to train the model, where  $\mathbf{x}$  denotes the input image,  $y$  denotes the corresponding true label, and  $\boldsymbol{\theta}$  denotes the parameters of the model.
2.  $\mathbf{h}_t$  denotes the output of  $t$ -th layer of the neural network.
3.  $s(\mathbf{h}_t)$  is the standard deviation of  $\mathbf{h}_t$ .

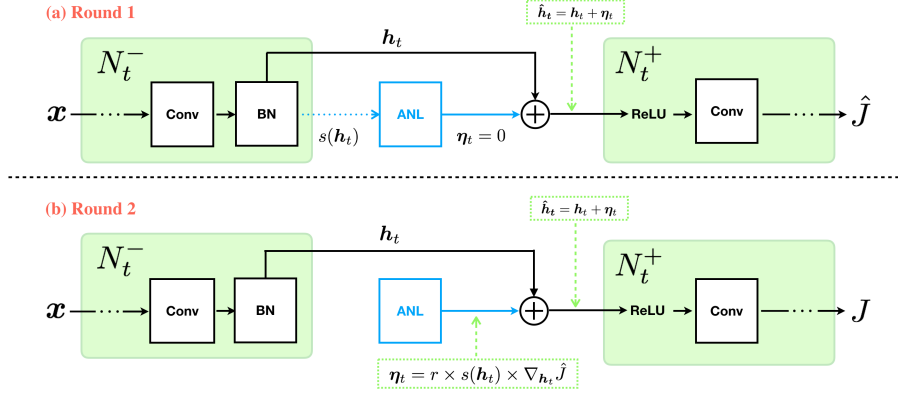


Figure 1: An illustration of two-rounds-training strategy. In the first round (a), ANL computes  $s(\mathbf{h}_t)$  in forward phase and  $\nabla_{\mathbf{h}_t} \hat{J}$  in backward phase. In the second round (b), ANL will generate noise in accordance with  $s(\mathbf{h}_t)$  and  $\nabla_{\mathbf{h}_t} \hat{J}$ , then the parameters of the network will be updated by back-propagation.

4.  $\eta_t$  is the adversarial noise for  $\mathbf{h}_t$ . Suppose the network has  $K$  layers, and we take the input as the 0 layer,  $\boldsymbol{\eta} \triangleq (\eta_0, \eta_1, \eta_2, \dots, \eta_K)^T$  denotes the entirety of the adversarial noise.
5.  $\epsilon$  is the hyper-parameter used to control the magnitude of noise for ANL.
6.  $\text{Clip}_{<a,b>}(\mathbf{v})$  denotes the element-wise clipping  $\mathbf{v}$ , with  $v_i$  clipped to the range  $[a, b]$ . If  $\mathbf{a}, \mathbf{b}$  are the same shape vectors as  $\mathbf{v}$ ,  $\text{Clip}_{<a,b>}(\mathbf{v})$  denotes clipping  $v_i$  to the range  $[a_i, b_i]$ .
7.  $\mathcal{N}(\mu, \sigma^2)$  denotes drawing a random sample from the Gaussian distribution where  $\mu$  is the mean and  $\sigma$  is the standard deviation (std).

### 3.2 Adversarial Noise Layer

The minimum distance to the decision boundary, which is regarded as the notation of margin, plays a foundational role in several profound theories and has empirically contributed to the overwhelming performance of both classification and regression tasks [23]. It is commonly believed that a robust image classification model has a large margin. Take linear classifier into consideration, the direction of gradient vector  $\nabla_{\mathbf{x}} J(\mathbf{x}, y)$  vertically points to the decision boundary, meaning that  $\hat{\mathbf{x}} \triangleq \mathbf{x} + \epsilon \nabla_{\mathbf{x}} J(\mathbf{x})$  is more close to the decision boundary than  $\mathbf{x}$ . Taking  $\hat{\mathbf{x}}$  to train will lead to higher cross-entropy loss and push the decision boundary away from  $\mathbf{x}$  more significantly, which helps to produce a larger margin classifier [1].

Similarly, we apply this idea to CNNs. The modern view of deep CNN architectures is that it extracts the vision features layer by layer [29]. We use  $\mathbf{h}_t$  to represent the output of  $t$ -th layer to analysis; denote the sub-network from the first layer to the  $t$ -th layer as  $N_t^-$ ; denote the sub-network from  $(t+1)$ -th layer to the last layer as  $N_t^+$ .  $\mathbf{h}_t$  is the output of  $N_t^-$  and the input of  $N_t^+$ .

Adding the specific perturbation  $\epsilon \nabla_{\mathbf{h}_t} J$  to  $\mathbf{h}_t$  leads to higher cross-entropy loss for  $N_t^+$ , which is also the loss for the whole network  $N$ . To reduce the loss, two changes will be conducted by back-propagation update. For the sub-network  $N_t^+$  which takes the  $\mathbf{h}_t$  as input, the update tends to push the boundary away from  $\mathbf{h}_t$ . For the sub-network  $N_t^-$  which generates  $\mathbf{h}_t$  as output, the update tends to push the  $\mathbf{h}_t$  away from the boundary. As result, the perturbation  $\epsilon \nabla_{\mathbf{h}_t} J$  instructs  $N_t^+$  to learn a larger margin classifier; instructs  $N_t^-$  to extract more distinctive features  $\mathbf{h}_t$  for different class  $\mathbf{x}$ . Considering these assumptions, we further propose Adversarial Noise Layer (ANL). ANLs simply add the adversarial noise  $\eta_t$  to  $\mathbf{h}_t$  and pass  $\hat{\mathbf{h}}_t$  to the next layer in the process of training.

$$\hat{\mathbf{h}}_t = \mathbf{h}_t + \eta_t \quad (1)$$

The noise is only added in training process. After the training process ends, the noise will be wipe out and  $\hat{\mathbf{h}}_t$  will be set as  $\mathbf{h}_t$  in inference phase. Therefore, ANL actually takes no extra computation in inference. The adversarial noise  $\eta_t$  is designed on the basis of the gradient of  $\mathbf{h}_t$ , enlarging the

margin of the decision boundary.

$$r = \text{Clip}_{<0, \epsilon>} \left\{ \mathcal{N} \left( \frac{\epsilon}{2}, \left( \frac{\epsilon}{4} \right)^2 \right) \right\} \quad (2)$$

$$\mathbf{g}_t = \nabla_{\mathbf{h}_t} J(\mathbf{x}, y; \boldsymbol{\theta}, \boldsymbol{\eta})|_{\boldsymbol{\eta}=0} \quad (3)$$

$$\boldsymbol{\eta}_t = r \frac{\mathbf{g}_t}{\|\mathbf{g}_t\|_\infty} \quad (4)$$

The random scalar  $r$  is used to control the magnitude of the noise. We find that CNNs models trained with dynamic magnitude noise obtain better performance than the models trained with the fixed magnitude. There are many possible distributions to draw a random sample  $r$  from. Here, we draw  $r$  from  $\mathcal{N}(\epsilon/2, (\epsilon/4)^2)$  since this Gaussian distribution requires only one hyper-parameter. Therefore, we have  $P(0 \leq r \leq \epsilon) = 95.4\%$ . Then we clip  $r$  to the range  $[0, \epsilon]$  to ensure  $r$  has been assigned a proper value. To simplify the usage of ANL, we use the same  $\epsilon$  for all Adversarial Noise Layers.

We trained VGG-16 network [21] on CIFAR-10 [8] with the adversarial noise calculated by Eq. (4). ANL is appended after every batch normalization layer [7], as illustrated in Figure 1. Figure 2(a) shows the standard deviation of the 13 ANL layers' input of the network. As it shows, the standard deviation differs from layer to layer and changes as the model converges. Considering the difference of standard deviation among layers, we multiply  $s(\mathbf{h}_t)$ , *i.e.* the standard deviation of  $\mathbf{h}_t$ , with  $r$  to adjust the magnitude of noise  $\boldsymbol{\eta}_t$  jointly. Therefore, we change the calculation of  $\boldsymbol{\eta}_t$  to:

$$\boldsymbol{\eta}_t = r s(\mathbf{h}_t) \frac{\mathbf{g}_t}{\|\mathbf{g}_t\|_\infty} \quad (5)$$

The Figure 2(b) shows the standard deviation of the VGG-16 network using Eq. (5). The insight of using  $s(\mathbf{h}_t)$  is that the noise should be bigger if the layer's output has relatively big standard deviation. The error rate of the VGG-16 network on CIFAR-10 drops from 6.53% to 5.91% by taking  $s(\mathbf{h}_t)$  into account while the error rate of the baseline model that trained without noise is 7.47%.

Training with ANL needs an extra forward and backward propagation to acquire the adversarial noise. We name this process as two-rounds-training strategy as shown in Figure 1. From it we can see that the adversarial noise is calculated after first back-propagation and the network is updated in second back-propagation (Algorithm 1).

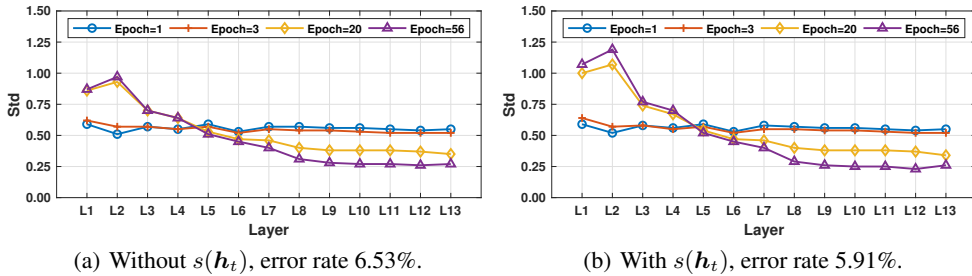


Figure 2: The comparison of the standard deviation for the input of 13 ANL layers with and without  $s(\mathbf{h}_t)$  under different epochs. (a) illustrates the network trained with the Adversarial Noise calculated by Eq. (4) and  $\epsilon = 0.025$ . (b) illustrates the network trained with the Adversarial Noise calculated by Eq. (5). Due to the  $s(\mathbf{h}_t)$  equals about 0.5 at beginning, we choose  $\epsilon = 0.05$  to eliminate the influence of scaling the magnitude of noise.

### 3.3 Adversarial Training is a Special Case of ANL

Goodfellow *et al.* introduced the method called Adversarial Training (AT) [1]. It generates a set of perturbed images by adding specific perturbation to the original data sample. Then, those perturbed images were merged with the original data set for training. AT can be denoted as follow:

$$\boldsymbol{\eta} = \epsilon \text{sign}(\nabla_{\mathbf{x}} J(\mathbf{x}, y; \boldsymbol{\theta})) \quad (6)$$

$$F(\mathbf{x}, y; \boldsymbol{\theta}) = J(\mathbf{x} + \boldsymbol{\eta}, y; \boldsymbol{\theta}) \quad (7)$$

---

**Algorithm 1** Training with ANL

---

**Require:**  $\epsilon > 0$ **repeat** $\eta \leftarrow 0$ calculate  $s(\mathbf{h}_t)$  through forward propagation $\mathbf{g}_t \leftarrow \nabla_{\mathbf{h}_t} J(\mathbf{x}, y; \boldsymbol{\theta}, \boldsymbol{\eta})$ **for**  $\eta_t$  in  $\boldsymbol{\eta}$  **do**pick  $r$  with Eq. (2)update  $\eta_t$  with Eq. (5)**end for**calculate the loss  $J(\mathbf{x}, y; \boldsymbol{\theta}, \boldsymbol{\eta})$  with adversarial noise  $\boldsymbol{\eta}$ update network with  $\boldsymbol{\theta} \leftarrow \boldsymbol{\theta} - \lambda \nabla_{\boldsymbol{\theta}} J(\mathbf{x}, y; \boldsymbol{\theta}, \boldsymbol{\eta})$ **until** training finish

---

where  $F(\mathbf{x}, y; \boldsymbol{\theta})$  is the new loss function. Therefore, it is viewed as training CNNs by adding an ANL only to the  $\mathbf{x}$ , of which the noise is calculated by:

$$\boldsymbol{\eta}_0 = \epsilon \text{sign}(\mathbf{g}_0) \quad (8)$$

where  $\mathbf{g}_0$  is the gradient of  $\mathbf{x}$  calculated by the first-round back-propagation and  $\boldsymbol{\eta}_0$  is the adversarial noise added to the  $\mathbf{x}$  in second-round forward propagation. It is concluded that AT can be regarded as a special case of ANL.

## 4 Experiments

We firstly do qualitative study on the ANL by analyzing the effects of different noise on feature maps. Then, we investigate the impact of hyper-parameter  $\epsilon$  and show high compatibility of ANL by conducting experiments in various mainstream CNN architectures. In the end, we verify the robustness of the model trained with ANL under the FGSM and IFGSM attack. Note that it is found that the models has fully-connected layers followed with ANL perform poorly. In our work, therefore, ANL is only implemented between convolution layers.

### 4.1 The Impact of Adversarial Noise

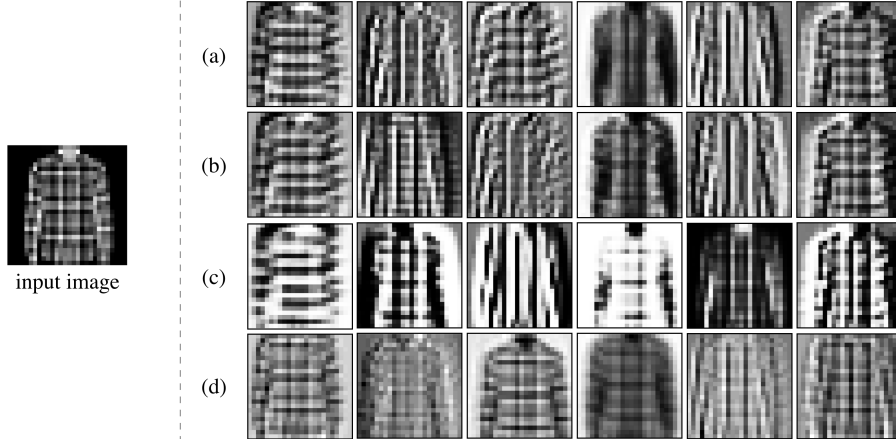


Figure 3: An illustration of feature maps from LeNet-5 [11] models trained with different noise. Each row represents the output of all 6 channels of the first convolutional layer. The left is the input image. (a) is the feature maps from the baseline network which is trained without noise. (b) is from the network trained with the Gaussian noise from  $\mathcal{N}(0, (\epsilon/4)^2)$  where  $\epsilon = 0.03$ . (c) is from the network trained with the Adversarial Noise where  $\epsilon = 0.03$ . (d) is from the network trained with the opposite of Adversarial Noise where  $\epsilon = -0.03$ .

Table 1: The test error (%) of LeNet-5 and VGG-16 trained with various noises.

Model	Dataset	Baseline	Gaussian Noise	+ANL $\epsilon = 0.03$	+ANL $\epsilon = -0.03$
Lenet-5	Fashion-MNIST	9.44	9.49	<b>9.17</b>	12.00
VGG-16	Fashion-MNIST	5.93	5.96	<b>5.47</b>	7.02
VGG-16	CIFAR-10	7.47	7.62	<b>6.18</b>	55.49

It is a straightforward way to illustrate the impact of adversarial noise by analyzing the feature map calculated by the convolutional layer. We demonstrate the experiment with the LeNet-5<sup>1</sup> [11] network on Fashion-MNIST [25] dataset. Firstly, we trained four Lenet-5 models with different types of noises respectively on Fashion-MNIST dataset under same initialization condition. Then we wipe out all of the noise layers and extract the output of the first convolution layer, put them through a sigmoid function to get the feature map images. Figure 3 shows the feature maps of the image from the test dataset.

According to the Figure 3, compared with the baseline, it is observed that the Gaussian noise make little difference while adversarial noise have apparent impact on feature extraction for the network. In addition, the feature maps with adversarial noise has sharper skeleton and structure, which indicates the model with adversarial noise tends to learn more distinctive features from input images. It is also found that adding opposite adversarial noise, *i.e.*, with negative  $\epsilon$ , tends to blurred feature maps severely, which leads to a tremendous score drop in our test.

The quantitative comparison is shown in Table 1. As it shows, we also explored the impact of different noises on VGG-16 [21] model on Fashion-MNIST and CIFAR-10 datasets. The VGG-16 models are initialized with same weights. It is observed that only adversarial noise with positive  $\epsilon$  improve the performance of the models while Gaussian Noise slightly degrades the models’ accuracy. In addition, we notice that the VGG-16 model trained with negative  $\epsilon$  achieves 99.6% accuracy on the train set of CIFAR-10 after few epoch, but the accuracy on test set is not higher than 44.51%. It is concluded that the opposite of adversarial noise results in tremendous degradation of performance.

## 4.2 Image Classification Task

Convolutional neural network is one of the most efficient tool in solving image classification task [4, 2, 27]. To identify proper value of  $\epsilon$  and investigate the compatibility of ANL, we compare the various CNN architectures trained with or without ANL on CIFAR-10 and CIFAR-100 dataset.

### 4.2.1 Experiment Settings

We follow the instruction of data augmentation mentioned in [13]: randomly performs horizontal flips, and takes a random crop with size 32x32 from images padded by 4 pixels on each side. The learning rate starts from 0.1 and would be divided by 2 until the most recent 5 epoch validation loss reach lower value than the best ever see. Each learning rate stays at least 5 epoch and the minimum of learning rate is 0.001. We use a weight decay of 5e-4 and momentum of 0.9 for all experiments. We train the baseline for 200 epoch. In comparison, the network is trained with ANLs for the first 100 epoch. Then we disable the ANLs and set the learning rate to the minimum (*i.e.* 1e-3) before we train the network for another 100 epoch.

We implement the ANL after each convolution layer or Batch Normalization [7] layer if it exists. We do not add the adversarial noise to input images due to it may cause slight degradation in accuracy. This problem will be addressed in section 4.3.

### 4.2.2 Classification Evaluation

**The choice of the hyper-parameter  $\epsilon$ .** To investigate the impact of different choices of the only hyper-parameter  $\epsilon$ , we train three different CNN models on CIFAR-10 with various  $\epsilon$ . According to Figure 4, the best choice of  $\epsilon$  varies from each other, mainly depending on the size of the network. The network with more trainable parameters performs better on relative large  $\epsilon$ . For example, the number of parameters of MobileNet-V2 is 2.3 million and its the best  $\epsilon$  is 0.02 while the best  $\epsilon$  for VGG-16 (14.7 million) is about 0.05. The best  $\epsilon$  for ResNet-18, which has around 11.2 million

<sup>1</sup>CONV-ANL-RELU-POOL-CONV-ANL-RELU-POOL-FC-RELU-FC-RELU-FC

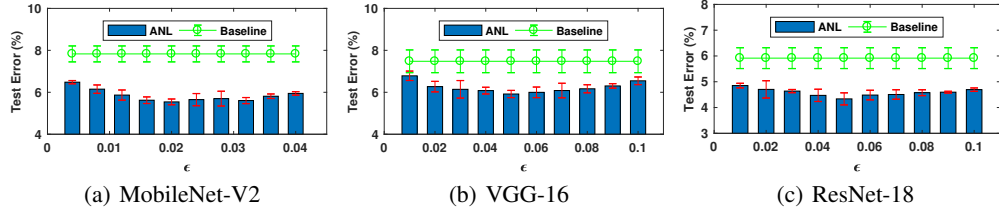


Figure 4: The test error(%) of (a) the MobileNet-V2 [20], (b) VGG-16 [21] and (c) ResNet-18 [4] on CIFAR-10, trained with different  $\epsilon$ .

Table 2: Test errors (%) with different architectures on CIFAR-10 and CIFAR-100 [8]. Baseline is the model trained without noise and dropout [22]. In (+Dropout), we insert dropout layers between convolutional layers and set drop ratio to 0.3 according to [27] for WRN. For the other networks, we insert dropout between FC layers and set drop ratio to 0.5 according to [5]. In (+ANL), we insert ANL after every batch normalization, and the choice of  $\epsilon$  is based on the amount of parameters of the network.

Model	#Params	$\epsilon$	Cifar10			Cifar100		
			Baseline	+Dropout	+ANL	Baseline	+Dropout	+ANL
MobileNet	3.20M	0.02	9.25	9.88	<b>7.84</b>	34.28	34.19	<b>30.71</b>
MobileNet v2	2.30M	0.02	7.83	7.86	<b>5.54</b>	29.64	30.70	<b>25.51</b>
VGG-11	9.20M	0.05	8.45	8.37	<b>7.67</b>	30.47	29.97	<b>29.19</b>
VGG-16	14.7M	0.05	7.47	7.16	<b>5.81</b>	29.45	28.91	<b>26.61</b>
ResNet-18	11.2M	0.05	5.98	5.03	<b>4.21</b>	24.16	22.83	<b>22.23</b>
ResNet-34	21.3M	0.08	5.34	4.70	<b>3.90</b>	23.42	22.14	<b>21.50</b>
PyramidNet-48	1.80M	0.01	5.62	5.16	<b>4.38</b>	25.14	25.24	<b>23.33</b>
PyramidNet-270	28.4M	0.10	4.68	4.10	<b>3.03</b>	19.55	18.94	<b>17.51</b>
WRN-40-4	8.90M	0.05	5.54	5.18	<b>3.56</b>	22.83	23.42	<b>21.31</b>
WRN-28-10	36.5M	0.10	4.10	4.07	<b>2.86</b>	21.37	20.90	<b>18.16</b>

trainable parameter, is also close to 0.05. The explanation for this phenomenon is that the network with more parameters is able to tolerate the larger noise while keep the representation power.

**Classification accuracy on different architectures and datasets.** To show the compatibility of ANL in various architectures, we trained various models with and without the ANL on the CIFAR-10 and the CIFAR-100 dataset. Six architectures are adopted: MobileNet [6], MobileNet v2 [20], VGG [21], ResNet [4], PyramidNet [2], and Wide Residual Networks(WRN) [27]. We also compared ANL with dropout. As shown in Table 2, comparing with baseline, the CNN models with ANL obtain better performance by a large margin. Also, the models with ANL obtains better performance than the models with dropout. In addition, ANL can be integrated together with most other regularization methods, which will be discussed in future.

### 4.3 Adversarial Attack Evaluation

Deep convolutional neural networks are easily fooled by careful designed adversarial examples. Plenty of literatures [1, 15, 10, 14] show that small perturbations cause well-designed deep networks to misclassify the image easily. In our experiment, we use the Fast Gradient Sign Method (FGSM) [1] and the Iterative Fast Gradient Sign Method (IFGSM) [10] to generate adversarial examples.

Assuming the input image  $x$  is in the range 0 to 255, the perturbed image using FGSM  $\hat{x}$  is generated as  $\hat{x} = x + \delta \text{sign}(\nabla_x J(x))$ . The value of  $\delta$  is usually set to small number relative to 255 to generate the perturbations imperceptible to human but degrade the accuracy of a network significantly. For IFGSM, this process is slightly modified as  $\hat{x}^k = \text{Clip}_{x-\delta, x+\delta}(\hat{x}^{k-1} + \alpha \text{sign}(\nabla_{\hat{x}^{k-1}} J(\hat{x}^{k-1})))$  where  $\hat{x}^0 = x$ ,  $k$  is the number of repeat iteration step in the process and it should satisfy  $k \geq \delta/\alpha$ .

To set up the testing for FGSM and IFGSM, we take two networks called the source network and the target network. We generate a set of perturbed images on the source network with FGSM or IFGSM and then measure the accuracy of the targeted network on these images. When the source and the target

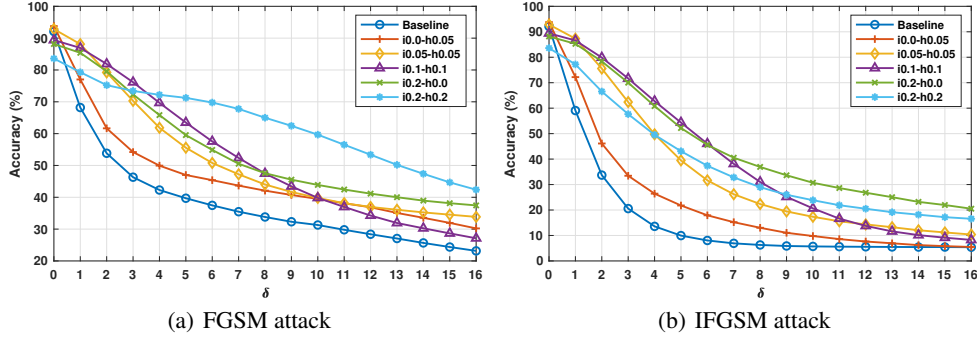


Figure 5: An illustration of test accuracy(%) of VGG-16 models trained with different noise on CIFAR-10 under the white box attack. (a) is the result for FGSM attack [1] with  $\delta = 16$ . (b) is the result for IFGSM attack [10] with  $\delta = 16, k = 16, \alpha = 1$ . Model code name  $i0.0 - h0.05$  stands for the  $\epsilon$  for the ANL-to-input is 0, the  $\epsilon$  for the ANLs-to-hidden is 0.05.

Table 3: The test accuracy(%) of models on the perturbed images generated by different models base on CIFAR-10. S stands for the source model, T stands for the target model. The number with underline is white box attack results; the rest is black box attack results. The last column is the test accuracy of original images. Model code name  $\begin{bmatrix} 0 \\ 0.05 \end{bmatrix}$  stands for the  $\epsilon$  for the ANL-to-input is 0, the  $\epsilon$  for the ANLs-to-hidden is 0.05.

S \ T		FGSM $\delta = 16$						IFGSM $\delta = 16, k = 16, \alpha = 1$						clean
		$\begin{bmatrix} 0 \\ 0 \end{bmatrix}$	$\begin{bmatrix} 0 \\ 0.05 \end{bmatrix}$	$\begin{bmatrix} 0.05 \\ 0.05 \end{bmatrix}$	$\begin{bmatrix} 0.1 \\ 0.1 \end{bmatrix}$	$\begin{bmatrix} 0.2 \\ 0 \end{bmatrix}$	$\begin{bmatrix} 0.2 \\ 0.2 \end{bmatrix}$	$\begin{bmatrix} 0 \\ 0 \end{bmatrix}$	$\begin{bmatrix} 0 \\ 0.05 \end{bmatrix}$	$\begin{bmatrix} 0.05 \\ 0.05 \end{bmatrix}$	$\begin{bmatrix} 0.1 \\ 0.1 \end{bmatrix}$	$\begin{bmatrix} 0.2 \\ 0 \end{bmatrix}$	$\begin{bmatrix} 0.2 \\ 0.2 \end{bmatrix}$	
$\begin{bmatrix} 0 \\ 0 \end{bmatrix}$	$\begin{bmatrix} 0 \\ 0 \end{bmatrix}$	<u>23.2</u>	29.1	64.0	65.6	79.6	62.9	<u>5.40</u>	44.4	83.0	84.1	86.2	77.8	92.54
$\begin{bmatrix} 0 \\ 0.05 \end{bmatrix}$	$\begin{bmatrix} 0 \\ 0.05 \end{bmatrix}$	35.9	<u>30.2</u>	55.6	62.0	76.4	60.9	13.2	<u>5.50</u>	72.1	79.2	84.5	74.0	<b>94.11</b>
$\begin{bmatrix} 0.05 \\ 0.05 \end{bmatrix}$	$\begin{bmatrix} 0.05 \\ 0.05 \end{bmatrix}$	35.7	36.4	<u>33.9</u>	50.3	60.2	52.5	13.8	14.0	<u>10.4</u>	36.2	62.3	44.6	92.92
$\begin{bmatrix} 0.1 \\ 0.1 \end{bmatrix}$	$\begin{bmatrix} 0.1 \\ 0.1 \end{bmatrix}$	22.9	23.9	28.5	<u>27.1</u>	48.5	38.7	8.50	8.90	12.2	<u>8.30</u>	41.7	21.8	89.78
$\begin{bmatrix} 0.2 \\ 0 \end{bmatrix}$	$\begin{bmatrix} 0.2 \\ 0 \end{bmatrix}$	48.9	51.5	45.0	53.6	<u>37.5</u>	54.3	33.4	36.7	34.9	41.3	<u>20.5</u>	45.5	89.08
$\begin{bmatrix} 0.2 \\ 0.2 \end{bmatrix}$	$\begin{bmatrix} 0.2 \\ 0.2 \end{bmatrix}$	25.0	25.3	38.1	45.0	61.1	<u>42.4</u>	37.0	41.4	54.1	57.5	71.5	<u>16.6</u>	83.60

network are the same, we name it white-box attack; when they are different, we name it as black-box attack [10]. (not sure grammar is right here.)

We trained six different VGG-16 networks on CIFAR-10 for the white-box and black-box attack. We not only add ANLs after the convolution layers (ANLs-to-hidden) but also add adversarial noise to the input  $x$  (ANL-to-input). The baseline are trained without noise and the other models are set with different  $\epsilon$ . Model code name  $i0.0 - h0.05$  or  $\begin{bmatrix} 0 \\ 0.05 \end{bmatrix}$  stands for the  $\epsilon$  for the ANL-to-input is 0, *i.e.* noise-free, the  $\epsilon$  for the ANLs-to-hidden is 0.05.

The results of the white-box attack of these models are shown in Figure 5 and the transfer rate of adversarial examples can be found in Table 3. All models trained with adversarial noise is more robust to the white box attack than baseline. The models are trained with larger noise tend to be more robust against attack. If we only add ANLs to the hidden layers, the model  $\begin{bmatrix} 0 \\ 0.05 \end{bmatrix}$  outperforms baseline significantly by 1.57% improvement on clean images. Adding the adversarial noise to the input will enhance the robustness to against FGSM and IFGSM attack but degrade the model’s performance on clean images. Compared with the model model  $\begin{bmatrix} 0 \\ 0.05 \end{bmatrix}$ , the accuracy of  $\begin{bmatrix} 0.05 \\ 0.05 \end{bmatrix}$  on clean images drops from 94.11% to 92.92%, but performs better on white / black box attack. The experiments suggest that adding adversarial noise with proper  $\epsilon$  into the hidden layers is always helpful for training robust CNN models. To keep security against adversarial examples, adversarial noise are added into the input images with relative big  $\epsilon$  improve robustness of CNN models against the attack though may result in the slight decrease of accuracy on clean data.



## 5 Conclusion

In this paper, we proposed a novel regularization algorithm named "Adversarial Noise Layer" to improve the generalization of CNNs. It is easy to implement and can be integrated with most of the CNN-based models. The ANL has only one hyper-parameter  $\epsilon$  and the choice of  $\epsilon$  is related to the number of parameters of the neural network. The adversarial noise is only added in training process, so there is no extra computation cost for CNN models in the inference phase. The model trained with ANL proved to be more robust under FGSM and IFGSM attack.

Currently, we only apply ANL in the image classification task. In the future work, we will explore other computer vision tasks such as the object detection and the face recognition. It is also interesting to explore the application of ANL in the area beyond computer vision, like the Nature Language Processing and the Voice Recognition.

## References

- [1] Goodfellow, I. J., Shlens, J., and Szegedy, C. (2015). Explaining and harnessing adversarial examples. *ICLR*.
- [2] Han, D., Kim, J., and Kim, J. (2017). Deep pyramidal residual networks. *CVPR*.
- [3] He, K., Gkioxari, G., Dollár, P., and Girshick, R. B. (2017). Mask R-CNN. In *ICCV*.
- [4] He, K., Zhang, X., Ren, S., and Sun, J. (2016a). Deep residual learning for image recognition. In *CVPR*.
- [5] He, K., Zhang, X., Ren, S., and Sun, J. (2016b). Identity mappings in deep residual networks. In *ECCV*.
- [6] Howard, A. G., Zhu, M., Chen, B., Kalenichenko, D., Wang, W., Weyand, T., Andreetto, M., and Adam, H. (2017). Mobilenets: Efficient convolutional neural networks for mobile vision applications. *arXiv preprint arXiv:1704.04861*.
- [7] Ioffe, S. and Szegedy, C. (2015). Batch normalization: Accelerating deep network training by reducing internal covariate shift. In *ICML*.
- [8] Krizhevsky, A. and Hinton, G. (2009). Learning multiple layers of features from tiny images.
- [9] Krizhevsky, A., Sutskever, I., and Hinton, G. E. (2012). Imagenet classification with deep convolutional neural networks. In *NIPS*, pages 1097–1105.
- [10] Kurakin, A., Goodfellow, I., and Bengio, S. (2017). Adversarial machine learning at scale. *ICLR*.
- [11] LeCun, Y., Bottou, L., Bengio, Y., and Haffner, P. (1998). Gradient-based learning applied to document recognition. *Proceedings of the IEEE*, 86(11):2278–2324.
- [12] Lee, C., Xie, S., Gallagher, P. W., Zhang, Z., and Tu, Z. (2015a). Deeply-supervised nets. In *AISTATS*.
- [13] Lee, C.-Y., Xie, S., Gallagher, P., Zhang, Z., and Tu, Z. (2015b). Deeply-supervised nets. In *Artificial Intelligence and Statistics*, pages 562–570.
- [14] Moosavi-Dezfooli, S., Fawzi, A., Fawzi, O., and Frossard, P. (2017). Universal adversarial perturbations. In *CVPR*.
- [15] Papernot, N., McDaniel, P., Goodfellow, I., Jha, S., Celik, Z. B., and Swami, A. (2017). Practical black-box attacks against machine learning. In *ASIACCS*.
- [16] Plaut, D. C. et al. (1986). Experiments on learning by back propagation.
- [17] Qian, R., Tan, R. T., Yang, W., Su, J., and Liu, J. (2017). Attentive generative adversarial network for raindrop removal from a single image. *arXiv preprint arXiv:1711.10098*.
- [18] Rosenblatt, F. (1957). *The perceptron, a perceiving and recognizing automaton Project Para*.
- [19] Russakovsky, O., Deng, J., Su, H., Krause, J., Satheesh, S., Ma, S., Huang, Z., Karpathy, A., Khosla, A., Bernstein, M. S., Berg, A. C., and Li, F. (2015). Imagenet large scale visual recognition challenge. *IJCV*, 115(3):211–252.
- [20] Sandler, M., Howard, A., Zhu, M., Zhmoginov, A., and Chen, L.-C. (2018). Inverted residuals and linear bottlenecks: Mobile networks for classification, detection and segmentation. *arXiv preprint arXiv:1801.04381*.
- [21] Simonyan, K. and Zisserman, A. (2015). Very deep convolutional networks for large-scale image recognition. *ICLR*.
- [22] Srivastava, N., Hinton, G., Krizhevsky, A., Sutskever, I., and Salakhutdinov, R. (2014). Dropout: A simple way to prevent neural networks from overfitting. *JMLR*, 15(1):1929–1958.
- [23] Vapnik, V. N. (1995). The nature of statistical learning theory.
- [24] Wan, L., Zeiler, M., Zhang, S., Le Cun, Y., and Fergus, R. (2013). Regularization of neural networks using dropconnect. In *ICML*.
- [25] Xiao, H., Rasul, K., and Vollgraf, R. (2017). Fashion-mnist: a novel image dataset for benchmarking machine learning algorithms. *arXiv preprint arXiv:1708.07747*.

- [26] Xie, L., Wang, J., Wei, Z., Wang, M., and Tian, Q. (2016). Disturblabel: Regularizing cnn on the loss layer. In CVPR.
- [27] Zagoruyko, S. and Komodakis, N. (2016). Wide residual networks. In BMVC.
- [28] Zeiler, M. D. and Fergus, R. (2013). Stochastic pooling for regularization of deep convolutional neural networks. ICLR.
- [29] Zeiler, M. D. and Fergus, R. (2014). Visualizing and understanding convolutional networks. In ECCV.
- [30] Zhong, Z., Zheng, L., Kang, G., Li, S., and Yang, Y. (2017). Random erasing data augmentation. arXiv preprint arXiv:1708.04896.